(Received 27 August 2024, Accepted 23 September 2024, Scheduled 3 October 2024)

Compact 2×1 Polarization Reconfigurable Dielectric Resonator Antenna Array Using Adaptable Feeding Network

Yazeed M. A. Qasaymeh*

Department of Electrical Engineering, College of Engineering, Majmaah University, Majmaah 11952, Saudi Arabia

ABSTRACT: In this paper, a compact 2×1 dielectric resonator antenna (DRA) array with circular polarization (CP) agility array is presented. The array is formed of two novel resonating elements, and each is composed of a pentagonal slot (PS) coupling a rectangular dielectric resonator (RDR). The proposed resonating element emits two degenerate orthogonal modes $TE^{x}_{\delta 11}$ and $TE^{y}_{\delta 21}$, confirming the CP radiation performance. The proposed resonator is utilized to portray a 2×1 sequentially rotated (SR) array with the ability to alter the CP polarization orientation. The signal at the feeding network input splits into two paths with equal magnitudes and phase progression phase by means of Wilkinson power divider (WPD). To obtain the 90 phase shifting between the WPD output signals, a single branchline coupler (BLC) is utilized. Considering the fact that the shifting orientation of the BLC output depends on which of the two BLCs is used as in input, the signal phase at the BLC can be controlled to yield a right hand circular polarization (RHCP) or left hand circular polarization (LHCP). To control the switching between the BLC output ports phase state, two PIN diodes are used at the BLC input ports. The $50 \times 50\,\text{mm}^2$ archetype achieves a bandwidth of 5.17% with a maximum realized gain of 7 dBic and a polarization purity of 4.4%. The findings of the proposed array make it a decent candidate for application using a 5.8 GHz band.

1. INTRODUCTION

Dual circular polarization (DCP) antennas offer various advantages such as competing multipath fading signals, enhancing system capacity, and battling polarization mismatch [1]. Such characteristics of DCP antenna make it a decent candidate for various wireless communication systems [3]. Technical considerations should be taken into account for designing DCP antennas such as high ports isolations and low cross polarization levels [2].

Richtmeyr in 1938 showed that the dielectric materials can function as electrical resonators at high frequencies [4], whilst the first practical DRA was presented by long et al. (1983) [5]. Since then, it gained the researchers attention due to its appealing features such as small size, various shapes, being triggered with different schemes and formed into an array [6]. Among different array topologies, SR feeding technique represents a good match for CP arrays as its main advantage is its ability to enhance the axial ratio (AR) bandwidth and the symmetry of the radiated fields [7].

The literature on DCP DRAs focuses on designing a single element antenna. Lim and Leung (2008) [8] presented a $120 \times 120\,\text{mm}^2$ prototype operating at 2.4 GHz. The design utilizes an underlaid hybrid coupler to excite two differential ports within a rectangular dielectric resonator (RDR) for DCP operation with AR bandwidth of 2.3–2.7 GHz. The design suffers from bulky size and design complexity. Zhao et al. (2020) [9] presented a $150 \times 150\,\text{mm}^2$ antenna utilizing an L-shaped slot and a vertical metal strip excitation scheme. A bowtie shape DRA consisting of two triangular dielectrics is used to for dual-sense CP operation. The proposed design achieves an impedance bandwidth of 63.7% and 3-dB polarization purity of 27.1 for RHCP and 12.8 for LHCP. The antenna's large size, design complexity, and unsymmetrical operation are major drawbacks. Li and Leung (2013) [10] proposed a DCP DRA prototype fabricated on a circular laminate of diameter of 49 mm. The design used a cylindrical dielectric resonator antenna (DRA) with a top-loaded modified Alford loop excitation scheme. The dual CP operation is obtained by controlling the branches of the Alford loop clockwise for RHCP and counterclockwise for LHCP. The achieved impedance bandwidth was 13.2% (2.34–2.67 GHz) with the gain of 1.8 dBic at 2.4 GHz. The polarization purity for port 1 was 5.3% (2.38–2.51 GHz) and 6.9% (2.39–2.56 GHz) for port 2. The unsymmetrical performance and design complexity are major disadvantages. Lu et al. (2016) [11] reported a dual feed exciting a T-shaped dielectric resonator (DR). The $21.5 \times 16.5\,\text{mm}^2$ antenna achieves a maximum gain of 3.3 dBic with impedance bandwidths of 17.2% (4.98–5.92 GHz) and 17.9% (5.02–6.03 GHz) for RHCP and LHCP, respectively. However, the complexity of feeding mechanism and low gain performance are major drawbacks.

Considering the aforementioned designs, a DRA array with dual senses of circular polarization is very idealistic. In light of above considerations, the goals of this communication are twofold. Proposing a novel resonating element that emits a CP radiated fields is the first goal. Hence, a pentagonal slot coupling a RDR with microstrip feed is proposed. The required mathematical background related to the proposed resonating element needs to be verified. Also, a detailed parametric study shall be carried out to exposure the proposed resonator funda-

* Corresponding author: Yazeed M. A. Qasaymeh (y.qasaymeh@mu.edu.sa).

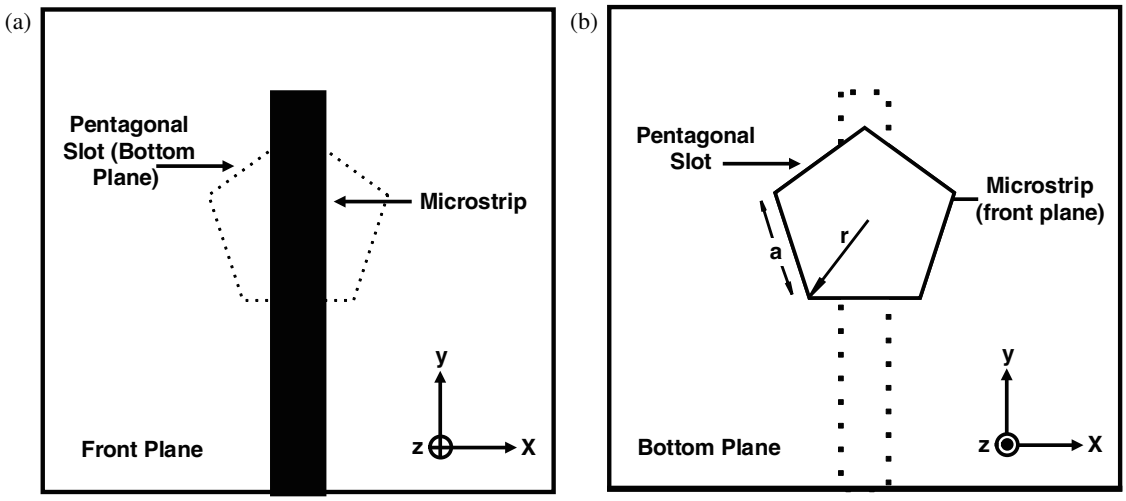

FIGURE 1. Topology of proposed resonator element (a) front plane (b) bottom plane (The RDR, mounted above the pentagonal slot, omitted to better visualize the coupling scheme).

mentals. Once the first goal is attained, feeding topology is assumed to acquire dual CP functionality. Henceforth, a novel feeding geometry is assumed using a single WPD, single BLC, and two PIN diodes to form a 2×1 array. Hence, the geometry of proposed feeding network needs to be clarified and discussed.

The presented communication is ordered as follows. In Section 2, the layout of proposed resonating element is provided with highlighting the mathematical background related to resonator sub-elements. A detailed parametric study is provided in Section 3 to unveil the proposed resonator fundamentals for optimum performance. In Section 4, the array feeding archetype is elaborated in order to highlight the achievement of DCP radiation. The obtained results are detailed and discussed in Section 5. Lastly, the conclusions and recommendations are included.

2. PROPOSED CP RESONATING ELEMENT

Figure 1 shows the proposed resonating element that consists of a pentagonal slot coupling a rectangular dielectric resonator at the bottom plane and a microstrip feed at the front plane. The microstrip slot coupling topology is chosen in this design due its several advantages, such as the slot formed into various profiles, the isolation between the radiation element and feeding network, and minimal cross polarization levels [12]. Also, for reconfigurable DRA design, the slot coupling technique provides a good isolation between the radiating DR and the feeding network which can avoid unwanted radiation performance deterioration. To provide full description of the proposed resonating antenna element, a three dimensional representation is depicted in Figure 2.

The pentagonal slot shape was selected because of its good input impedance matching, good radiation characteristics, optimized area, and ease of reactive loading as compared to other open slot-based designs. The main advantage of pentagonal slot amongst other polygon shapes, which has a better performance in terms of bandwidth, realizes gain and occupies less space than circular antenna [13]. The resonance frequency of pentagonal slot antenna can be estimated using Equation (1) reported by [14].

$$f_{mn} = \frac{k_{mn} C}{4.649 a \sqrt{r_c}} \tag{1}$$

where c is the speed of light, k_{mn} the Bessel function coefficient, a the side length, and r_c the equivalent radius.

One of the major advantages of DRA is that it can be formed into variety of shapes including but not limited to cylindrical, spherical, and rectangular geometries. Amongst these shapes, the rectangular one is polygon shape which is preferable due its fabrication simplicity and offers the designer a degree of freedom as its three dimensions can be determined independently. In [15], a mathematical approximation can be used to estimate the RDR dimensions at specified resonance frequency according to Equations (1)–(4).

$$f_0 = \frac{15\left[a_1 + a_2\left(w/2h\right) + 0.16\left(w/2h\right)^2\right]}{w\pi\sqrt{\varepsilon_r}} \tag{2}$$

$$a_1 = 2.57 - 0.8\left(\frac{d}{2h}\right) + 0.42\left(\frac{d}{2h}\right)^2 - 0.05\left(\frac{d}{2h}\right)^3 \tag{3}$$

$$a_2 = 2.71\left(\frac{d}{2h}\right)^{-0.282} \tag{4}$$

where d, w, and h are the length, width, and height of the rectangular resonator respectively, and ε_r is the DR material dielectric permittivity.

3. PROPOSED RESONATOR PARAMETRICAL VERIFICATION

In order to clarify the aspects of proposed resonator, a prototype is modeled using Computer Simulation Technology (CST) microwave studio. Various parametrical seeps were performed on

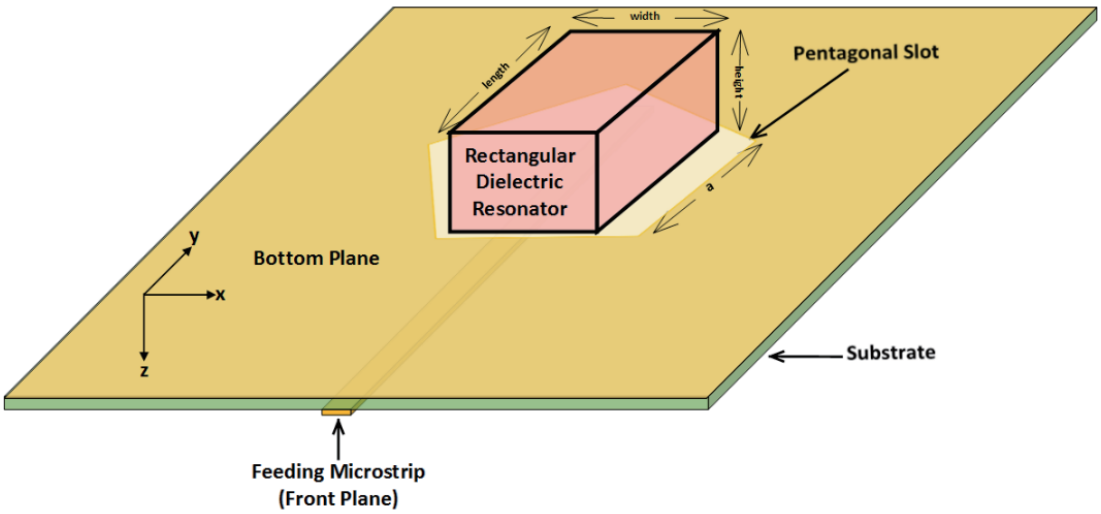

FIGURE 2. Three dimensional representation of proposed resonating antenna elements.

modeled prototype to elucidate the effect of proposed resonator physical dimensions to obtain a CP matched resonator. The influence of the RDR length, width, and height, as well as the pentagonal slot radius on resonance frequency, AR bandwidth, impedance matching and realized gain, are thoroughly investigated.

Figure 3 depicts the effect of altering the dimensions as well the pentagonal slot radius on the resonance attitude. The proposed resonator is fine tuned to operate at frequency of 5.8 GHz. The optimization is performed as altering one parameter while keeping the others unchanged. From various simulation sweeps, it is found that the resonance occurs at 5.812 GHz if the pentagonal slot radius is 5 mm, and the RDR length, width, and height are 10 mm, 10 mm and 9.5 mm, respectively.

Once the resonance performance is ensured, it is essential to confirm the resonator CP performance. Smith chart is a possible way to track the CP attitude of an antenna. According to [16], if there is a small loop at Smith chart, a CP radiation is confirmed. This is attributed to the fact that the loop on the Smith chart occurs if two resonance modes are trigged with the DR. In Figure 4, the impedance matching is represented at the optimal resonance frequency of 5.812 GHz. The small loop appears at the middle of the chart confirms the presence of CP radiation as well as a good impedance matching occurred near 50 Ω.

Another way to ensure the CP performance is to track the excited modes within the RDR boundaries. If two orthogonal modes are triggered within the DR, the radiated fields will be circularly polarized. For that purpose, Figure 5 depicts the electric fields with the DR in the xz and yz planes. From the figure, it can be inferred that the modes $\mathrm{TE}^{x}_{\delta 11}$ and $\mathrm{TE}^{y}_{\delta 21}$ are excited at the optimal resonance frequency.

4. ARRAY FEEDING TOPOLOGY

Figure 6 depicts the proposed feeding schematic for 2×1 polarized reconfigurable antenna. The feeding network is composed of a single WPD, two PIN diodes, and a single BLC. The square shape of the WPD is utilized as it provides more compactness to the design [17]. BLC is used in this design as its geometry allows the control of the phase at the output ports depending on which of the two input ports is utilized. Also, the BLC has various advantages, low profile, easy fabrication, and light weight to name just a few. For that, BLC is widely used for many microwave applications and integrated circuits [18]. Amongst various electrical switches components, the PIN diodes are used broadly compared to all other switches based on low insertion loss, good isolation, low power consumption, and low cost [19, 20]. A main advantage of the proposed array is its symmetrical geometry which would lead to symmetrical results for both polarization states.

Figure 7 depicts that the polarization states can be obtained by the proposed feeding network geometry. In Figure 7(a), at the WPD output ports, if PIN diode D1 is set to state OFF, the BLC input signal is only from PIN diode D2 path, resulting in a 90 phase shift at the BLC output port 1 and no phase shifting at BLC output port 2. Hence, an RHCP is obtained. The reversal procedure occurs if PIN diode D2 is set to OFF state resulting in an LHCP phase progression at the BLC output ports as described in Figure 7(b). Hence, a DCP operation is obtained utilizing only two PIN diodes, a single WPD, and single BLC. In Figure 7, the feeding geometry is explained at the array front side with the pentagonal coupling slot and RDR positioned on the bottom side of the array.

To validate the assumed current flow hypothesis, an array prototype is modeled using computer simulation technology (CST) microwave studio software, and the current progression phase is tracked as depicted in Figure 8. In Figure 8(a), PIN diode D1 is set to ON state only, and in Figure 8(b) only PIN diode D2 is set to ON state. By tracking the phase at the output ports, which couple the slots and RDR at the bottom plane, it can be observed that an RHCP is attained once D1 is conducting, and if D2 is set to ON state, an LHCP is achieved. Hence, the phenomena of acquiring a DCP operation is vali-

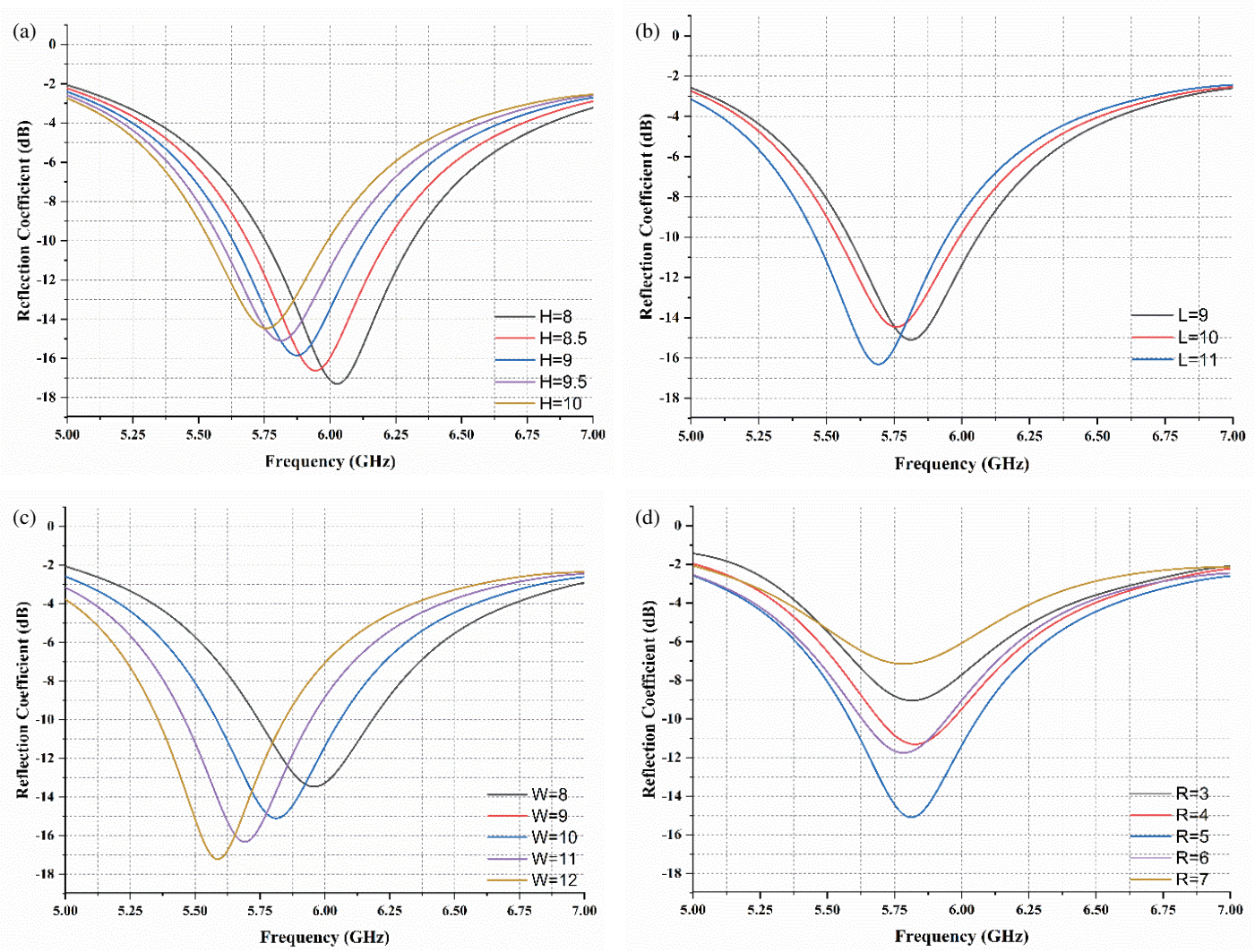

FIGURE 3. Effect of proposed resonator physical dissensions on resonance frequency. (a) RDR height. (b) RDR length. (c) RDR width and (d) pentagonal slot radius.

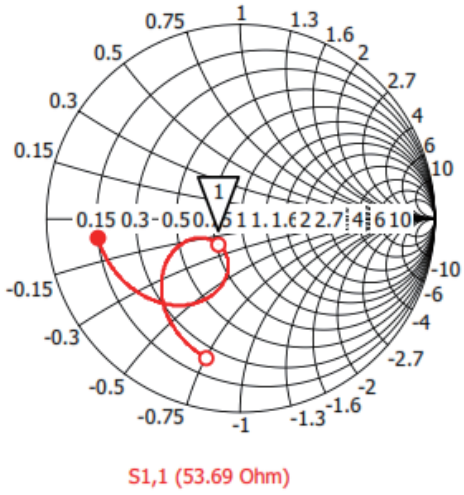

FIGURE 4. The impedance matching at the optimal resonance frequency.

dated. Moreover, from Figure 8, it is noticed that a sufficient amount of current is delivered to the radiating element at the bottom plane. For that, it is expected that a sufficient power is delivered, and consequently the gain performance is expected to be optimum.

5. RESULTS AND DISCUSSIONS

Figure 9 describes the fabricated DCP antenna array. The Alumina material with a dielectric constant of 9.8 is adopted to model the RDRs. Conversely, the laminate RO4003C of dielectric constant 3.38 and height of 0.813 mm from Rogers is executed to model the $30 \times 50 \times 0.813\,\text{mm}^3$ substrate. The PS and RDR dimensions are set as verified in Section 3 as 5 mm is the radius of the slot, and the RDR dimensions are $10 \times 10 \times 9.5\,\text{mm}^3$. The WPD and BLC are designed at an optimal frequency of 5.8 GHz. The WPD for each side length equals 7.03 mm or $\lambda/4$. Nevertheless, the divider arms width is set to 1.0539 mm to obtain an impedance of $\sqrt{2}Z_0$ as indicated in Figure 5(a). For the BLC, the coupler inner arm's length is

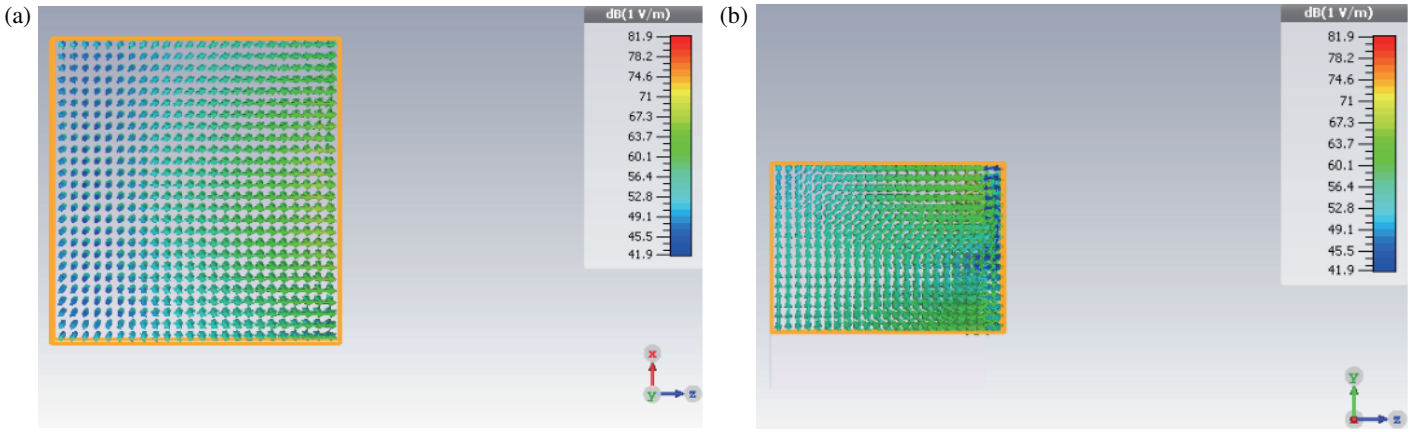

FIGURE 5. The excited modes within the RDR at (a) xz plane (b) yz plane.

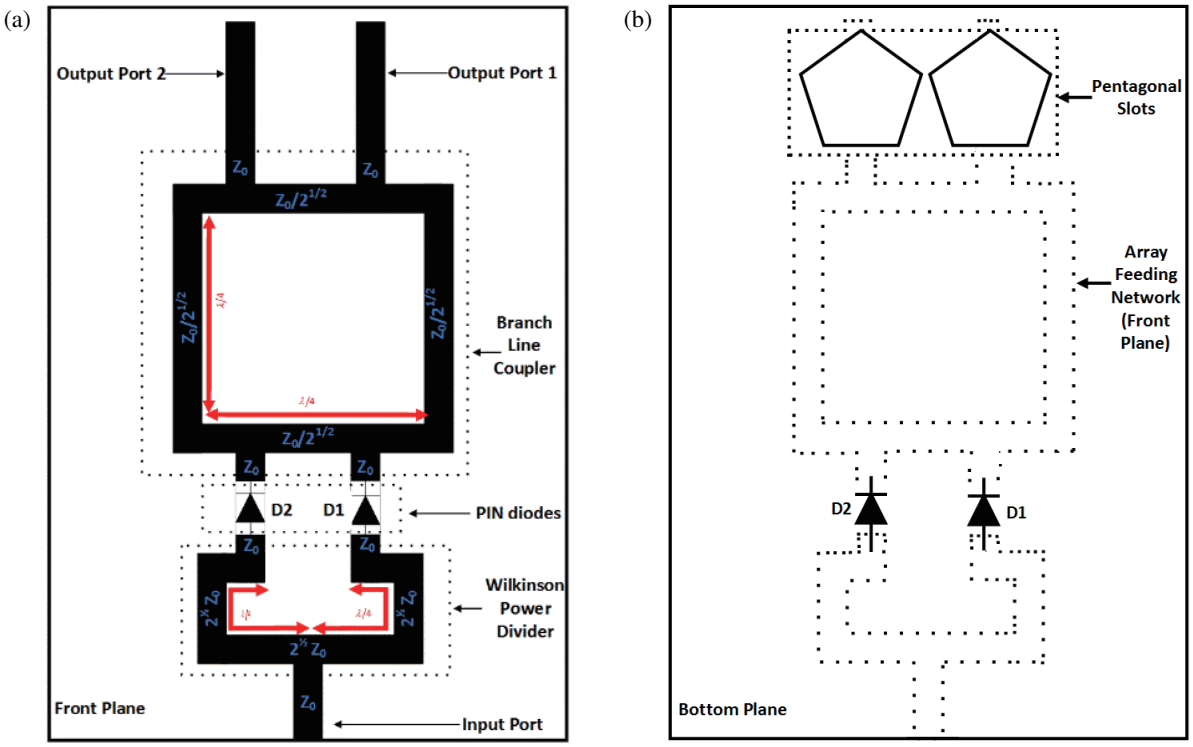

FIGURE 6. The proposed feeding geometry (a) front plane showing the impedance of each segment in blue and the related wave length in red (b) bottom plane showing the allocation of the slots with respect to feeding network on the front plane.

set to 7.03 mm or $\lambda/4$ as explained in Figure 5(a), whilst the arm width equals 1.5805 mm to obtain a 35.35 Ω. The front plane is etched with the feeding network, and the bottom plane is carved with the PSs. The RDR is positioned above the PSs. The current patch was managed by switches made with Infineon Technologies PIN diodes BAR63-02V. A pair of DC-blocking capacitors and a pair of chock inductors are manipulated to integrate each PIN diode.

Figure 10 unveils the simulated and measured reflection coefficients. As the array feeding is symmetrical, an identical result will be scored if either of the PIN diodes is set to ON state. The simulated impedance bandwidth ranges from 5.474 to 5.886 GHz with a minimal resonance taking place at 5.796 GHz of −27.13 dB. The measured ones range from 5.576 to 5.872 GHz with a minimal loss of −25 dB happening at 5.792 GHz. A minor disparity is observed between the simulated and measured results, stemming from fabrication losses, the influence of inductors and capacitors, and soldering inconsistencies. However, there is a reasonable level of concurrence between the two sets of outcomes.

Figure 11 exhibits the simulated and measured fields in the xz plane at the optimal resonance frequency of 5.8 GHz. In Figure 11(a), where the PIN diode 1 is ON state, and the co-polarized fields are higher than the cross-polarized ones.

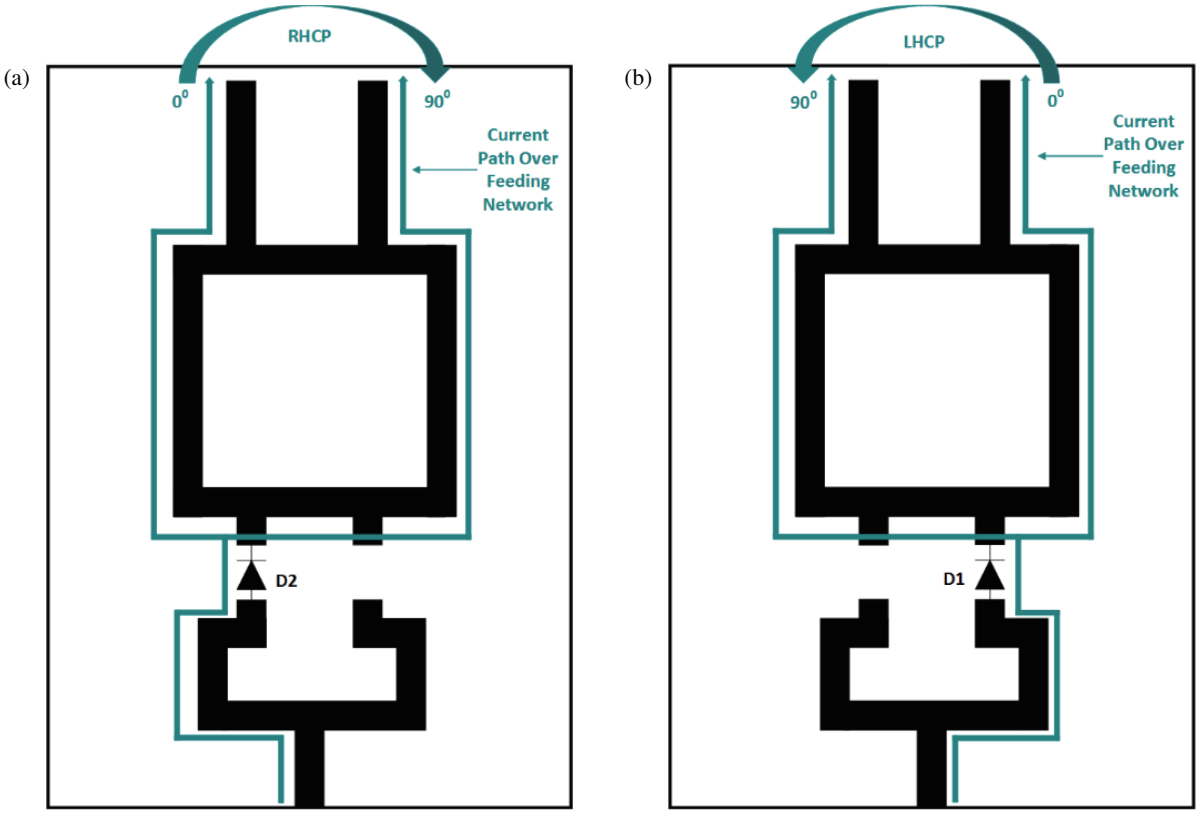

FIGURE 7. Phenomena of controlling the signal phase at the output ports. (a) RHCP is obtained if PIN diodes D1 is OFF (b) LHCP is obtained if PIN diodes D1 is OFF.

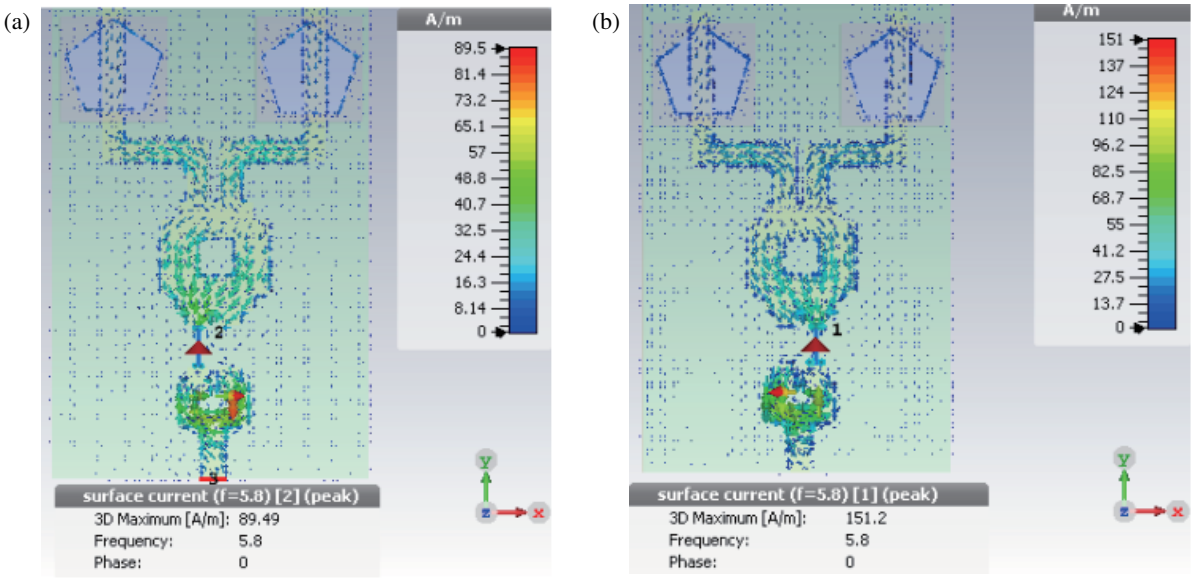

FIGURE 8. Current distribution over the feeding network: (a) PIN diodes 1 is ON State for RHCP; (b) PIN diodes 2 is ON state for LHCP.

Hence, an RHCP is achieved. On the other hand, in Figure 11(b), the cross-polarized fields are greater than the co-polarized patterns. Henceforth, an LHCP condition is fulfilled. These results affirm that the introduced feeding geometry is able to emit DCP operation. Generating comparable radiation patterns for both polarization states is a major benefit of the resulting fields, namely, symmetric array feeding. Moreover, a directive radiation is attained in the direction of the RDR ,and the back loop is minimal in the side of the feeding network. Finally, a good agreement is found between the simulation and measurement which is mainly attributed to accuracy in setting the simulation and measurement environment.

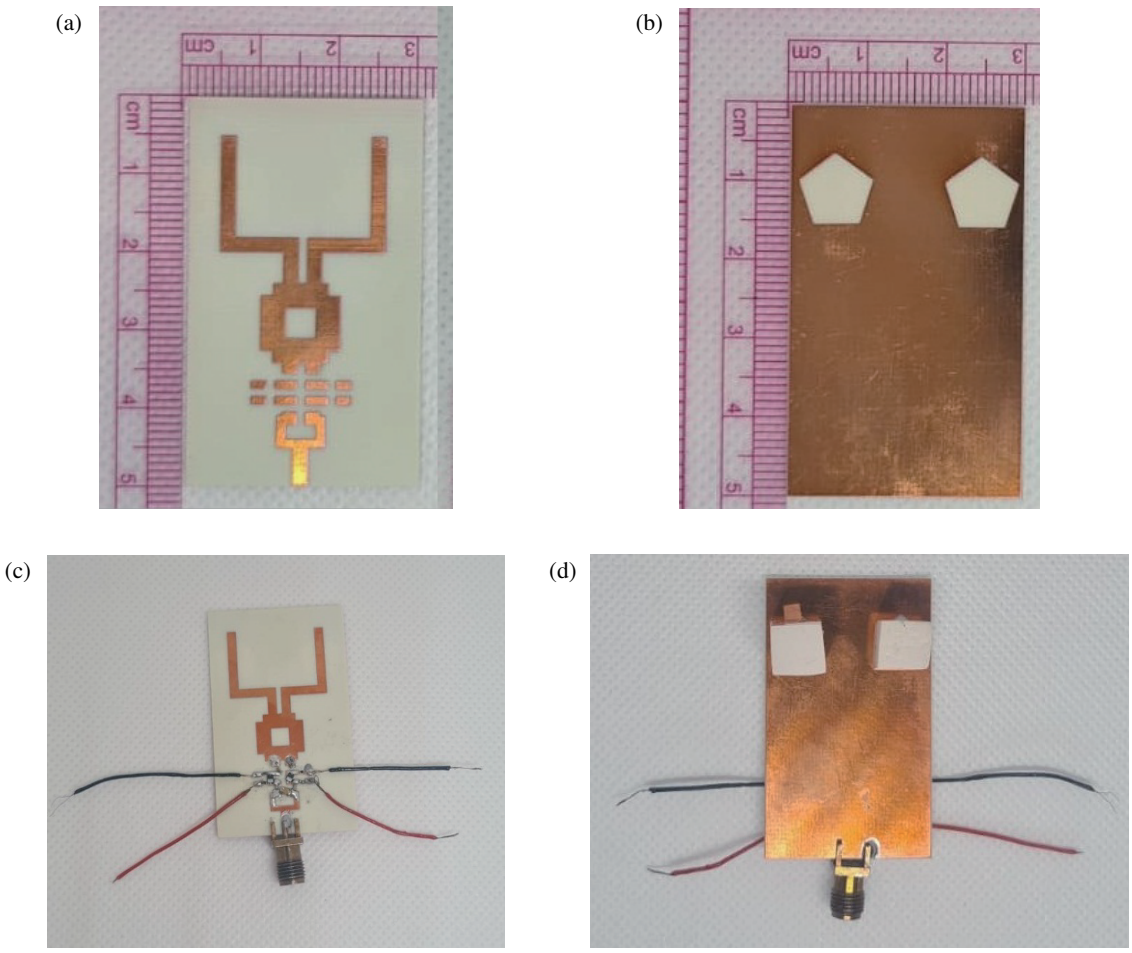

FIGURE 9. Developed prototype of the introduced antenna array: (a) front plane without integrating the PIN diodes; (b) front plane with integrating the PIN diodes; (c) bottom plane without mounting the RDRs; (d) bottom plane without mounting the RDRs above the PSs.

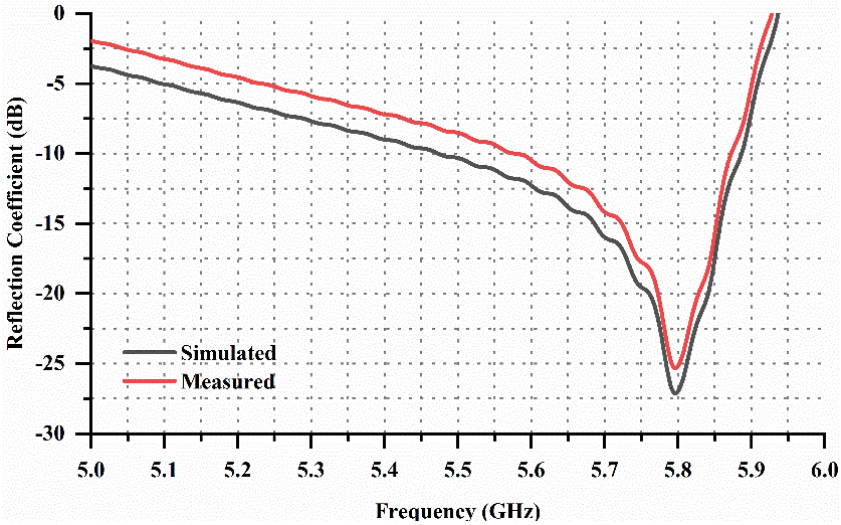

FIGURE 10. Simulated and measured reflection coefficients.

Figure 12 exposes the simulated and measured gains and efficiencies along the resonance band. A stable gain operation is acquired due to the symmetrical array geometry. A maximum measurement of gain nearly 7 dBi is obtained as normally a single-element DRA generates the gain around 5 dBi. A minor difference between the simulated and measured gains oc-

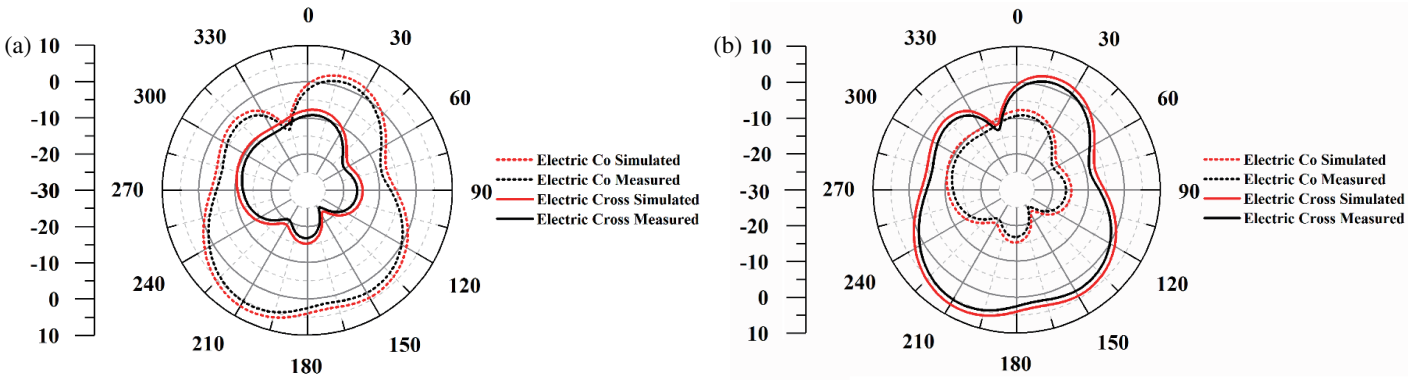

FIGURE 11. Simulated and measured radiated fields in the zx plane: (a) radiated field one D1 is ON state; (b) radiated field one D2 is ON state.

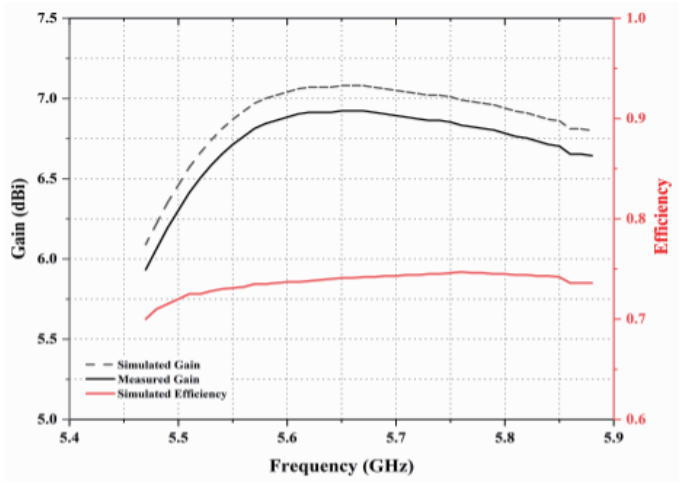

FIGURE 12. Simulated and measured gains variation of the proposed array.

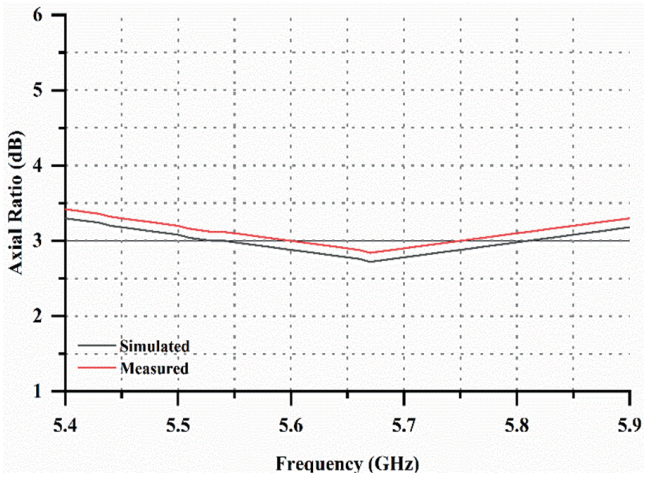

FIGURE 13. Simulated and measured axial ratio.

TABLE 1. Comparison between the proposed array and other DCP DRAs.

Reference	Size [mm^2]	Bandwidth %	Axial ratio %	Peak gain
[8]	120 × 120	4.1	16	Not mentioned
[9]	Not mentioned	63.7	27.1	Not mentioned
[10]	Circular substrate with a diameter of 49 mm	13.2	5.3	1.8 dBic
[11]	21.5 × 16.5	17.2	17.9	3.3 dBic
The proposed work	30 × 50	5.17	4.4	7 dBic

curs which is attributed to the cables and connectors losses due to the measurement setup. The gain performance will be enhanced if a reflector is installed beneath the feeding network of the array front plane.

Figure 13 discloses the simulated and measured polarization purity along the resonance bandwidth. Thus, it is concluded that the simulated AR bandwidth is 4.93% compared to 4.4% for measurement. The concurrence between the two results is fairly good.

6. CONCLUSIONS

In this paper, a novel 2×1 DCP DRA array is presented and experimentally validated. The array is formed of novel radiating elements; each is composed of a PS coupling an RDR on the bottom plane and excited by a microstrip fed at the front plane. The resonator subelements mathematical background is elaborated, and the resonator features are authenticated via parametrical study. Once the proposed resonator characteristics are verified by radiating CP fields, a feeding network is projected

to control the polarization sense. For that purpose, a simple feeding network containing a single WPD and single BLC is assumed. With the proper allocation of the PIN diodes, the current phase progression can be controlled and hence the array polarization sense. In Table 1, a comparison between other DCP DRAs in the literature and the proposed array is introduced. Both the gain boost and size decrease are discernible in the DRA array proposed in this paper. For future work, the design concept is applicable to other frequency bands as well as the array element number which can be increased for the aim of accomplishing higher gain and/or impedance bandwidth.

REFERENCES

[1] Mohit, K., V. R. Gupta, and S. K. Rout, "Two element magneto-dielectric resonator antenna for angle diversity," *Frequenz*, Vol. 70, No. 5-6, 203–210, 2016.

[2] Zhao, Z., J. Ren, Y. Liu, Z. Zhou, and Y. Yin, "Wideband dual-feed, dual-sense circularly polarized dielectric resonator antenna," *IEEE Transactions on Antennas and Propagation*, Vol. 68, No. 12, 7785–7793, 2020.

[3] Xu, H., Z. Chen, H. Liu, L. Chang, T. Huang, S. Ye, L. Zhang, and C. Du, "Single-fed dual-circularly polarized stacked dielectric resonator antenna for K/Ka-band UAV satellite communications," *IEEE Transactions on Vehicular Technology*, Vol. 71, No. 4, 4449–4453, 2022.

[4] Richtmyer, R. D., "Dielectric resonators," *Journal of Applied Physics*, Vol. 10, No. 6, 391–398, 1939.

[5] Long, S., M. McAllister, and L. Shen, "The resonant cylindrical dielectric cavity antenna," *IEEE Transactions on Antennas and Propagation*, Vol. 31, No. 3, 406–412, 1983.

[6] Mandal, S., A. De, and C. K. Ghosh, "Design and performance analysis of a compact, wideband dual polarized antenna for WLAN & WiMAX applications," *Frequenz*, Vol. 77, No. 1-2, 95–106, 2023.

[7] Luo, K., W. Ding, and W. Zhu, "Broadband circularly polarized cavity backed slot antenna array with broadband sequential rotation feed," *Frequenz*, Vol. 67, No. 11-12, 353–358, 2013.

[8] Lim, E. H. and K. W. Leung, "Compact wideband circularly polarized dielectric resonator antenna with an underlaid hybrid coupler," in *2008 IEEE Antennas and Propagation Society International Symposium*, 1–4, San Diego, CA, USA, Jul. 2008.

[9] Zhao, Z., J. Ren, Y. Liu, Z. Zhou, and Y. Yin, "Wideband dual-feed, dual-sense circularly polarized dielectric resonator antenna," *IEEE Transactions on Antennas and Propagation*, Vol. 68, No. 12, 7785–7793, Dec. 2020.

[10] Li, W. W. and K. W. Leung, "Omnidirectional circularly polarized dielectric resonator antenna with top-loaded Alford loop for pattern diversity design," *IEEE Transactions on Antennas and Propagation*, Vol. 61, No. 8, 4246–4256, 2013.

[11] Lu, L., Y.-C. Jiao, W. Liang, and H. Zhang, "A novel low-profile dual circularly polarized dielectric resonator antenna," *IEEE Transactions on Antennas and Propagation*, Vol. 64, No. 9, 4078–4083, 2016.

[12] Kumar, A., P. Kapoor, P. Kumar, J. Kumar, and A. Kumar, "Design and development of enhanced gain aperture coupled broadband biodegradable dielectric resonator antenna for WLAN applications," *Wireless Personal Communications*, Vol. 115, 1525–1539, 2020.

[13] Jose, J. A., R. Anand, S. Rao, and S. K. Menon, "A coplanar pentagonal antenna for wireless applications," in *2015 2nd International Conference on Signal Processing and Integrated Networks (SPIN)*, 40–43, Noida, India, 2015.

[14] Deshmukh, A. A. and V. A. P. Chavali, "Wideband pentagonal shape microstrip antenna using a pair of rectangular slots," *Progress In Electromagnetics Research C*, Vol. 107, 113–126, 2021.

[15] Wang, F., C. Zhang, H. Sun, and Y. Xiao, "Ultra-wideband dielectric resonator antenna design based on multilayer form," *International Journal of Antennas and Propagation*, Vol. 2019, No. 1, 4391474, 2019.

[16] Lu, J.-H., C.-L. Tang, and K.-L. Wong, "Single-feed slotted equilateral-triangular microstrip antenna for circular polarization," *IEEE Transactions on Antennas and Propagation*, Vol. 47, No. 7, 1174–1178, 1999.

[17] Ameen, M. and R. K. Chaudhary, "ENG-TL inspired dual-polarized antenna using curved meander, two-arm Archimedean spirals and CSRR mushroom," *Microwave and Optical Technology Letters*, Vol. 65, No. 6, 1778–1786, 2023.

[18] Jamshidi, M. B., S. Roshani, J. Talla, S. Roshani, and Z. Peroutka, "Size reduction and performance improvement of a microstrip wilkinson power divider using a hybrid design technique," *Scientific Reports*, Vol. 11, No. 1, 7773, 2021.

[19] Steer, M., *Microwave and RF Design: A Systems Approach*, 2nd ed., 180, SciTech Publishing, 2010.

[20] Yashchyshyn, Y., K. Derzakowski, G. Bogdan, K. Godziszewski, D. Nyzovets, C. H. Kim, and B. Park, "Suitability of S-PIN diodes used in reconfigurable antennas," in *2018 14th International Conference on Advanced Trends in Radioelecrtronics, Telecommunications and Computer Engineering (TCSET)*, 587–590, Lviv-Slavske, Ukraine, Feb. 2018.